Available online at www.sciencedirect.com
SCIENCE DIRECT®
Biosensors and Bioelectronics 18 (2003) 429–435
BIOSENSORS & BIOELECTRONICS
www.elsevier.com/locate/bios

Backside contacted field effect transistor array for extracellular signal recording

S. Ingebrandt [a,1], C.K. Yeung [a,2], W. Staab [b], T. Zetterer [b,3], A. Offenhäusser [a,*]

[a] Max-Planck-Institute for Polymer Research, Ackermannweg 10, D-55128 Mainz, Germany
[b] Institute for Microtechnology Mainz, Carl-Zeiss-Strasse 18-20, D-55129 Mainz, Germany

Received 31 October 2001; received in revised form 12 June 2002; accepted 31 July 2002

Abstract

A new approach to the design of field-effect transistor (FET) sensors and the use of these FETs in detecting extracellular electrophysiological recordings is reported. Backside contacts were engineered by deep reactive ion etching and a gas phase boron doping process of the holes using planar diffusion sources. The metal contacts were designed to fit on top of the bonding pads of a standard industrial 22-pin DIL (dual inline) chip carrier. To minimise contact resistance, the metal backside contacts of the chips were electroless plated with gold. The chips were mounted on top of the bonding pads using a standard flip-chip process and a fineplacer unit previously described. Rat embryonic myocytes were cultured on these new devices (effective growth area 6×6 mm^2) in order to confirm their validity in electrophysiological recording.

Keywords: Field effect transistor; Backside contact; Deep reactive ion etching; Gas phase doping; Extracellular recording; Rat cardiac myocyte

1. Introduction

Backside contacts to ion-sensitive field-effect transistors (ISFETs) have been fabricated in former studies (Van Den Vlekkert et al., 1988; Ewald et al., 1990; Merlos et al., 1995; Osorio-Saucedo et al., 1996). The advantage of such backside contacts is the easier encapsulation of the chips. In standard ISFET structures, the electric contacts to source and drain are fabricated by bonding of thin aluminium wires to the frontside of the devices followed by encapsulation of these wires with epoxy glue to prevent shortcuts. The major drawbacks of this procedure are the higher costs of this handmade encapsulation and the lower reliability in long term use. By reusing the devices, the epoxy begins to detach and the device starts to degrade.

Field-effect transistor (FET) arrays for the extracellular recording of signals from living cells have been developed and used in former studies (Fromherz, 1999; Fromherz et al., 1991; Offenhäusser et al., 1997; Sprössler et al., 1998). For all these devices, frontside contacts were used.

The combination of life cells with extracellular recording devices offers new perspectives for the development of whole-cell biosensor devices, which was first proposed by Regehr et al. (1989). Whole-cell biosensors may be used in a variety of research areas such as pharmacology, cell biology, toxicology, and environmental measurements. One particularly important application is drug discovery and screening. It is believed that these biosensor systems can replace some of the existing and well-established in vitro functional assays and can be used to complement other biochemical methods (e.g. ligand binding assays) in biomedical research.

One of the promising approaches is the use of cardiac myocyte cells cultured on transistors (Ingebrandt et al., 2001; Sprössler et al., 1999; Yeung et al., 2000, 2001). In

* Corresponding author. Present address: Institute for Thin Films and Interfaces (ISG2), Research Centre Jülich, D-52425 Jülich, Germany. Tel.: +49-2461-61-23330; fax: +49-2461-61-2333
E-mail address: a.offenhaeusser@fz-juelich.de (A. Offenhäusser).
[1] Present address: Institute for Thin Films and Interfaces (ISG2), Research Centre Jülich, D-52425 Jülich, Germany.
[2] Present address: Department of Ophtalmology and Visual Science, Chinese University Hong Kong, Hong Kong.
[3] Present address: Schott Telecom Optics GmbH, Mainz, Germany.

0956-5663/02/$ - see front matter
PII: S0956-5663(02)00155-0

order to obtain accurate, reliable and quantifiable response of the biosensor, it is very important to control the amount of drug being administered. One possible solution for the controlled administration is the adaptation of micro-mechanically engineered microflow-systems (Thiébaud et al., 2002). A major disadvantage of standard front-side contacted FET devices is the topology of the encapsulation caused by the wirebond contacts at the front-side of the device (Offenhäusser et al., 1997). In this article, we report a possible solution for this problem by micro-mechanically engineered backside contacts of the FET chips. The chips are contacted using standard flip-chip technology (Higgins et al., 1998; Jansseune and Brand, 1998; Lau, 1995). The metal pads of the devices are designed to fit on top of the wirebond board of a standard DIL socket. Rectangular glass rings are glued on top of these chip carriers forming a petri dish, which holds 700 μl of culture medium. The accessible surface area of the chips is 6×6 mm^2.

The transistor gates of the 16-channel backside contacted devices are arranged in a 4×4 FET array of 100 or 200 μm spacing. The backside contacts were fabricated using deep reactive ion etching (DRIE) (Douglas, 1989; Laermer and Schilp, 1999; Stern and Medeiros, 1992) and a gas phase boron doping process (Powell, 1987). At the front-side of the chips, the electrical contacts are protected against the electrolyte by a thin free-standing layer of silicon dioxide and silicon nitride over the holes.

The noise level of these devices is slightly higher than the noise level of similar front-side contacted devices, mainly caused by the higher drain- and source-resistors as a result of the backside contact. However, this did not interfere with the recording of extracellular signals from a beating cardiac myocyte layer cultured on the sensor surface. The backside contact offers new encapsulation methods such as upside down devices, where the sensor is manoeuvred on top of cell cultures already established on standard tissue culture dishes.

2. Materials and methods

2.1. Fabrication procedures

In a first step double sided polished n-doped silicon (phosphorus doped, $1 \times 10^{15}/cm^3$; $\rho = 8.5–11.5\ \Omega$ cm) was oxidised in wet atmosphere to form the field oxide ($d_{ox} \approx 1$ μm). In the following step, the photographically defined lane contacts on the front-side were implanted with boron ($D = 8 \times 10^{15}/cm^2$). In a diffusion step followed by a wet-oxidation process, the depth of the pn-junction (source and drain) was adjusted to about 4 μm ($R_\gamma = 13.2\ \Omega_\gamma$). The oxide layer ($d_{ox} \approx 1$ μm), which was produced in this step, is part of the layer which covers later the hole and acts in addition as etching stop for the DRIE process of silicon (Douglas, 1989; Laermer and Schilp, 1999; Stern and Medeiros, 1992). In the second implantation step, the gate dimensions were defined followed by a second diffusion/oxidation step (Fig. 1A).

After opening the gate areas and deposition of a thin (70 nm) oxide as etching stop in the gate area (Offenhäusser et al., 1997), a 380 nm thick silicon nitride film (LPCVD, low-pressure chemical vapour deposition, 790 °C) was deposited onto the whole wafer. This unusually thick silicon nitride layer was required in order to compensate the mechanical stress of the SiO_2/Si_3N_4 layer system that is formed above the areas wherein the next process step holes are etched from the backside.

In the following steps, the backside of the wafer was processed. In a photolithographic step, the outer lane area at the backside was opened through the nitride layer in a reactive ion etching (RIE) process. The remaining oxide layer was removed in a wet etching process using HF acid solution (Fig. 1B).

In the next photolithography step, the roundshaped holes at the backside were defined. The diameters of the

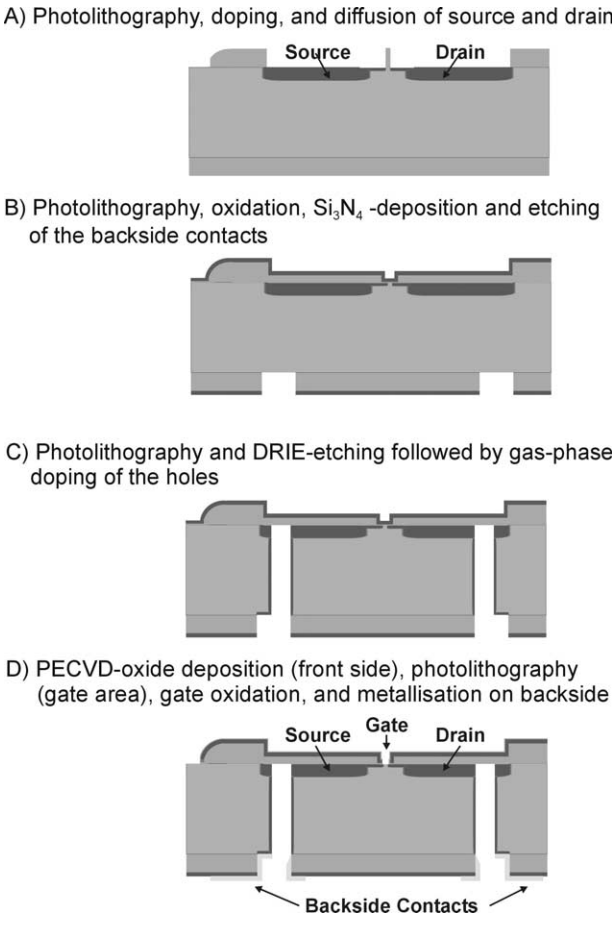

Fig. 1. Main fabrication steps for the devices (not to scale).

holes are 100 μm at the outer wafer area and 150 μm at the inner wafer area, because the etching rate of the DRIE process was not the same over the wafer area. The photoresist at the backside was used as mask layer for the DRIE-process for the production of the holes through the wafers. This silicon etching process was a two step cycle process (duty 10 s) with reactive etching and deposition of passivation material at the walls (Douglas, 1989; Laermer and Schilp, 1999; Stern and Medeiros, 1992). The oxide layer at the front-side acted as etchstop for this process. In this step, it was crucial to avoid underetching in order not to de-stabilise the free-standing layer system on top of the holes. From this step on, the wafers had to be handled with extreme care, because the free-standing oxide/nitride layer system had a total thickness of only 1.44 μm and a diameter of about 150 μm. In order to produce electrical contact from the backside to the front-side, the holes were doped using a gas phase process (Fig. 1C) (Powell, 1987) using BN-/Si-wafers in sandwich configuration at 950 °C. This diffusion resulted in a layer resistance of $R = 100\ \Omega$ at the backside contacts and a resistance through the holes of ca. 200–250 Ω.

Following the contact-hole formation process, the final fabrication steps at the wafer front-side were performed. First, a PECVD-layer (plasma enhanced chemical vapour deposition) of 100 nm thick silicon oxide was deposited as passivation and to enhance the compatibility with standard cell culturing protocols. In the next photolithographic step, the gate windows were opened and the gate oxide was grown in a dry-oxide process ($d_{ox} = 10$ nm) (Fig. 1D).

In the last step, the metal contacts at the backside were produced. For the use of the transistor arrays in a flip-chip process, it was found that gold contacts are essential for obtaining good contact resistances in the mΩ range (Simon and Reichl, 1990). First, the metallic contacts to the p-doped silicon were produced by sputtering 1 μm aluminium (with 1% Si). Then the front-side was shielded with a polyimide layer and the aluminium was pre-etched for the preparation of electroless metal deposition. After this, a precursor of zincate solution (NaOH, ZnO, HNa-tartrate, KNO_3, $FeCl_3$) produced nucleation centres at the aluminium surface. The electroless deposition of nickel and gold was performed following the procedure described by Simon and Reichl (1990) (Fig. 2). After removing the polyimide from the front-side, the wafers were diced and the chips were ready for encapsulation.

2.2. Device assembly and encapsulation

Besides the wider open areas of the chip, one main advantage of the backside contacts is that no wirebonding to the chips is necessary. The contacts are established with the flip-chip technique (Higgins et al., 1998; Jansseune and Brand, 1998; Lau, 1995). The design of the metal contacts at the chip backside is adapted to the dimensions of a 22 pin DIL chip carrier (Spectrum Semiconductor Materials Inc., San Jose, USA) and the chips are directly mounted on top of the gold-plated bonding pads of the chip carrier (Fig. 4). The second main advantage is the simplified chip encapsulation, which is performed after gluing a rectangular glass ring on top of the chip carrier and lining up the bath chamber with PDMS glue (SYLGARD 96-083, Dow Corning, Germany). The use of an isolating epoxy underfill (Underfill U300, Epoxy Technology Inc., USA) prevents shortcuts between the flip-chip bumps (Higgins et al., 1998). In addition, the membranes of the chips are stabilised by the underfill epoxy glue which is dragged into the holes by capillary forces.[4] The flip-chip process was done with a combination of screen-printer and fineplacer set-up described before (Krause et al., 2000) and the use of two-component flip-chip epoxy glue (EPO-TEK H20E-PFC, Epoxy Technology Inc., USA). The optical controlled fineplacer unit (FINEPLACER-145 'PICO', FINTECH Electronic, Germany) offers a very high planar accuracy.

The chip-layout of the backside-contacted FET-arrays is shown in Fig. 3. The design of the lanes is adapted to the largest lane area to reduce series resistance of the drain and source contacts. The topology of the device is almost flat, which is important for cell density control when cells are being plated onto the surface.

2.3. Cell culture

Cardiac myocytes from embryonic (embryonic day 18, E18) Sprague–Dawley rats were used. The myocytes were prepared using previously described dissociation techniques (Denyer et al., 1999; Krause et al., 2000). The hearts of about eight embryos were used for one culture. The cells were plated onto the fibronectin-coated devices (5 μg/ml). The total number of cells per chip was adjusted to be 40–60,000 at the time of cell seeding. After 4 days in culture the cells formed a homogeneous layer, which spontaneously contracted with a stable frequency.

2.4. Measurement set-up

The housing of the preamplifier headstage was designed to work with an upright microscope in the reflection mode equipped with differential interference

[4] Due to the wetting properties, the underfill closes holes down to several μm in diameter. In addition, the incorporation of air bubbles can be avoided by turning the assembly up-side-down so that air can escape.

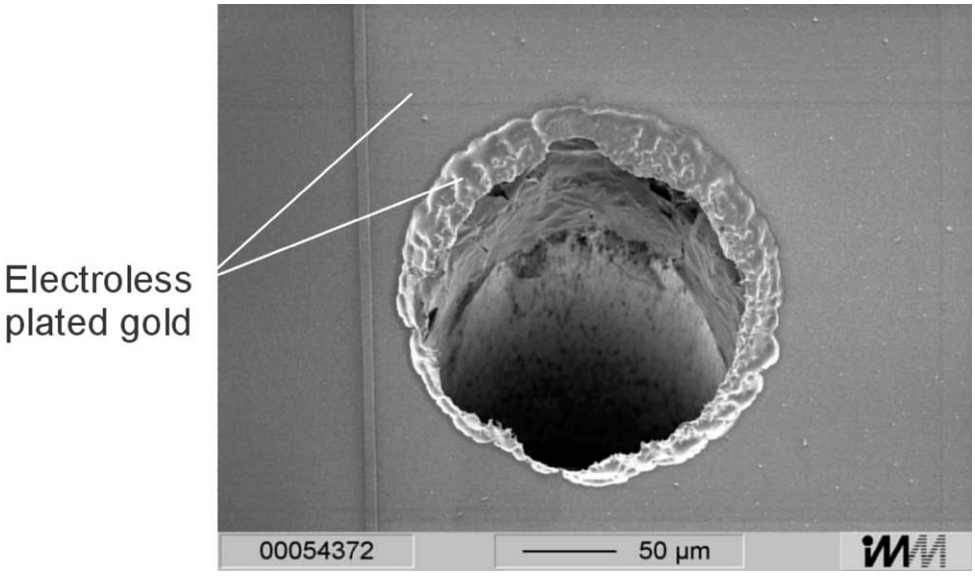

Fig. 2. SEM image of an etched hole on the backside contacted chip. The backside contacts were electroless plated with gold.

contrast (DIC) optic. A zero force socket in the housing enables a quick change of the FET-devices. The electronic circuitry of the preamplifier headstage is similar to the circuitry used in the headstage of the standard devices (Sprössler et al., 1998). Briefly, in the first step the drain-source current is converted to a voltage ($U = 10$ kΩ I) and in a second step the obtained voltage is compensated for all offset components and further amplified by a factor of 100. In order to be compatible with electrophysiological recording systems (e.g. patch-clamp amplifier), the reference electrode (Ag/AgCl-electrode), which acts as gate contact, is set to ground potential. For extracellular measurements, the 16-channel amplifier system with a battery based power supply described in Krause et al. (2000) was used.

3. Results

In Fig. 5, the electrical characteristic of a typical transistor layout are shown. Fig. 5a shows a typical output-, Fig. 5b a transfer- and Fig. 5c a transconductance-characteristics using a chip with a gate size of 2×38 µm^2. It can be seen that the transistor can be operated at a maximum transconductance (normalized to the channel width) of $g_m = 9.5$ µS/µm in the working point $V_{GS} = -2.5$ V, $V_{DS} = -3$ V. In this working point, the total noise level at the gate input of the FETs was measured to be about 200 µV (peak-to-peak), which can be seen in Fig. 6 (e.g. channel 1). For the different gate designs, a transconductance of 6 µS/µm and a noise level of about 250 µV (peak-to-peak) represent average values.

Cardiac myocytes were cultured on the sensor surface for 4 days before recordings. In Fig. 6, a typical recording using the 16-channel FET sensor is shown. The cells were beating spontaneously and the electrical activity of the cells was monitored online. The interpretation of the extracellular signal shapes has been discussed previously (Sprössler et al., 1999; Krause et al., 2000; Ingebrandt et al., 2001). In total 10 out of 16 channels in this particular measurement showed extracellular signals of the beating cell layer. The trace measured with channel 10 reflects the noise level of the

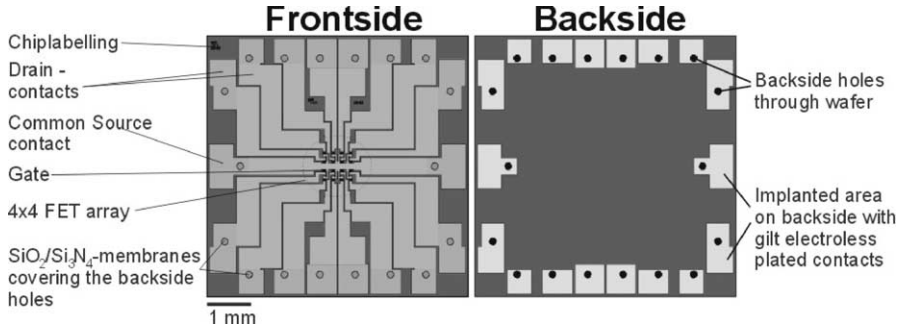

Fig. 3. Layout of the FET arrays. The 4×4 FET array has a common source contact and 16 individually addressable drain contacts. The standard spacing of the FET gates at the front-side of the chips is 100 and 200 µm.

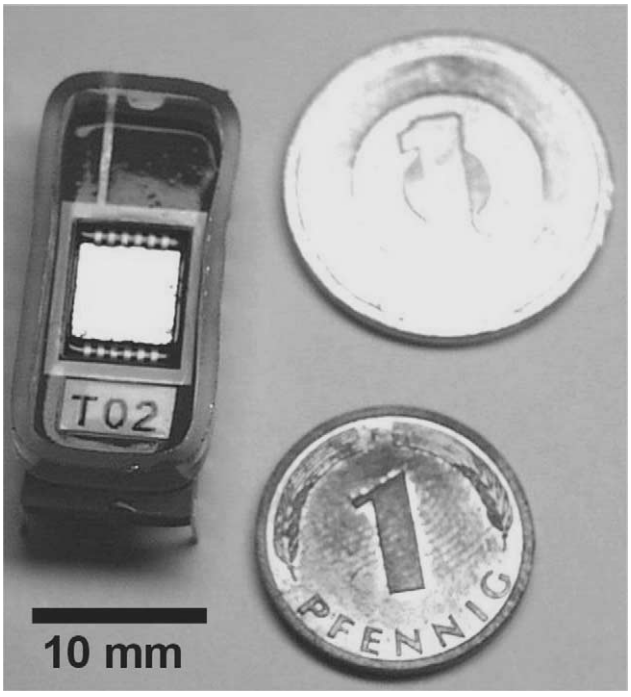

Fig. 4. Encapsulated backside contacted FET device. The upper coin is a Japanese 1 Yen and the lower one, a German 1 Pfennig are shown for comparison.

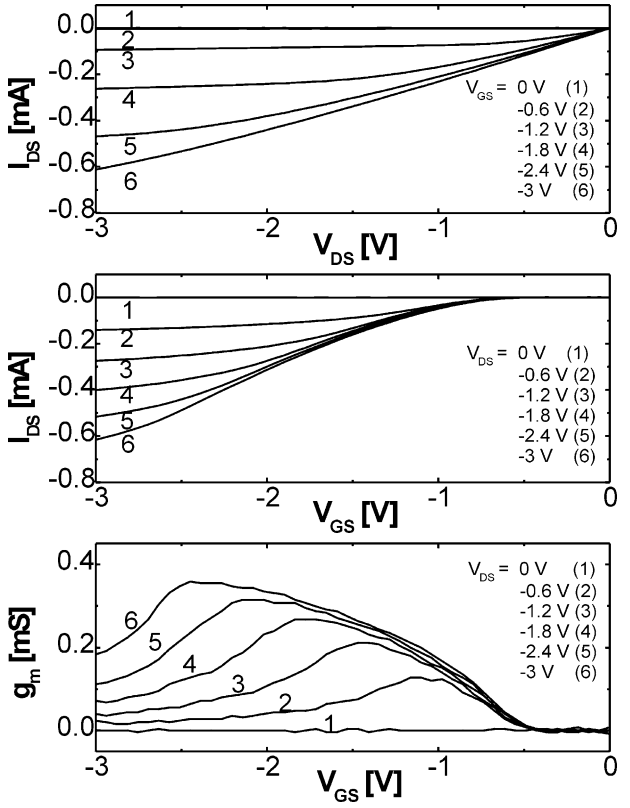

Fig. 5. Characteristics of the device: (a) output-; (b) transfer-; and (c) transconductance-characteristics of the FET devices.

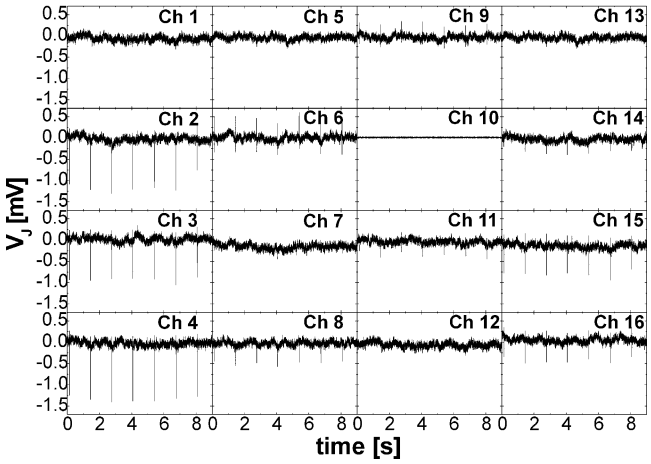

Fig. 6. Signals from a spontaneously beating cardiac myocyte cell layer (4 DIV) on a backside contacted FET device.

amplifier set-up without the transistor structure at the input, as this channel had no electrical contact with the transistor array. By comparing the noise level of this channel with the noise level of the working transistors, it can be seen that the transistor acts as main noise source in the amplification cascade (Sprössler et al., 1998).

The amplitudes of the extracellular signals recorded in this particular measurement are ranging from 1.5 (channel 4) to 0.3 mV (channel 14). This relatively high deviation of the signal-to-noise ratios ($S/N = 7.5$–1.5) is caused by the difference of the cell-transistor contacts at the single sensor spots. The amplitudes of the extracellularly recorded signals are strongly correlated to close contacts and very high sealing resistances of the cell layer at the transistor gates.

Fig. 7 shows the details of one action potential recorded with channel 4. The signal shape differs from the shape of the intracellular recorded action potential as it can be recorded using e.g. patch-clamp electrodes. As it was discussed previously, the observed FET-signals can be divided into three major categories A, B, and D (Sprössler et al., 1999). The categories A and B are based only on the contribution of the passive elements of the

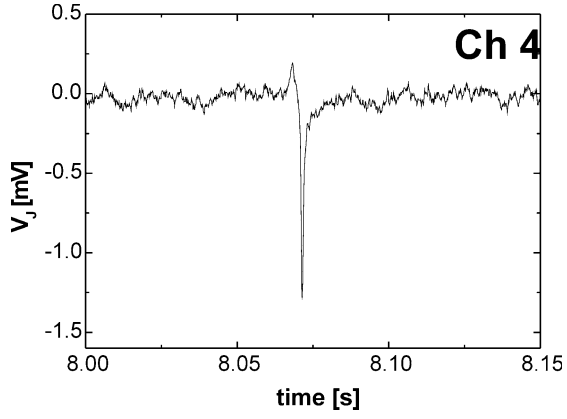

Fig. 7. Details of an action potential recorded with channel 4.

cell membrane in contact with FET, whereas signals with contribution of the ion current flow across the cell membrane in contact with the FET can be subcategorized in D1–D4. Subtype D1 describes a signal where all membrane currents in the contact area are proportional to the membrane currents through the rest of the cell. Subtype D2 and D3 describe situations where the Ca-current is comparatively enhanced and dominates the extracellular signal. Subtype D4 shows a major contribution of K-current in the contact area. It should be noted that the most frequent recordings are categorized in subclass D1 and that the subclasses D2–D4 are usually observed with a frequency below 5%. The positive upstroke at the beginning of the signal (Fig. 7, D1-type) can be attributed to the stimulus current injected by neighbouring cells. The fast negative spike is due to a recorded Na^+ ion current. Fig. 7 does not show any major contribution of Ca^{2+} and K^+ ion currents in the junction area between cells and sensor.

In order to simulate the different signal shapes, we described the coupling of the cells to the FET-sensor by using the point-contact model (Regehr et al., 1989; Fromherz et al., 1991; Sprössler et al., 1999). By considering a simple equivalent circuit, it is possible to describe the principles involved in the recording using FETs. The separation of the cell membrane and the gate results in an extended cleft of electrolyte which can be described by a specific conductance. The membrane region beneath the transistor as well as the free part of the membrane is described by a specific membrane capacitance. Incorporated in this membrane are various channels with time- and voltage-dependent and independent specific ionic conductances contributing to the current through the membrane. By neglecting other contributions (ion sensitivity of the device, mechanical signals due to contraction of the cells), the extracellular voltage V_J is determined by Kirchhoff's law. Therefore, the extracellular signal can be described as a combination of the charging current of the membrane capacitance (which is proportional to the derivative of the membrane voltage) and the ionic current through the attached membrane.

It was shown that almost the complete extracellular signal (except the stimulation spike at the beginning) would diminish if one would not assume other influences. Such a possible effect for the description of the extracellular signals is the assumption of different ion current densities through the free and the attached membrane due to different opening properties or different channel densities. However, there has been to our knowledge no final proof for this concept. Another possible explanation could be the ion-sensitivity of the open gate FETs in the physiological buffer regime (Ingebrandt, 2001). The effect of the mechanical contractions of the cardiac myocytes seem to have almost no influence on the extracellular signal: on the one side the mechanical contractions appear clearly (several 10 ms later) after the sodium peak current which gives the major contribution to the extracellular signal, on the other side it was shown by decoupling the electrical and the mechanical signals that there was almost no influence visible.

4. Conclusion

A backside contacted 16-channel FET device for the measurement of extracellular signals has been developed. The concept of the backside contact offers new encapsulation and mounting methods by using the flip-chip technique. The new chip offers a much larger surface area for a variety of cell cultures, such as standard dissociated or tissue slices. Due to the planar structure of the device (including encapsulation etc.) it would even be possible to obtain electrophysiological recordings with this type of sensor chips being placed directly on cells cultured on standard petri dishes or even from tissues by lowering the chips on top of the cells.

The FETs show a classical transistor characteristics with a maximum transconductance of 9.5 μS/μm. With the FET device it was possible to record extracellular signals from cardiac myocyte layers cultured on fibronectin primed sensor surfaces.

Acknowledgements

We would like to thank Professor Dr W. Knoll (Max-Planck-Institute for Polymer Research) for his support. Mr. Müller and Mr. Richter from the electronic-workshop, Mr. Gerstenberg and Mr. Christ from the mechanic-workshop of the MPI for Polymer Research are acknowledged for excellent technical support. This work was funded by the Ministerium für Bildung, Wissenschaft, Forschung und Technologie (BMBF), German Ministry of Science and Technologie (Project No. 0310895).

References

Denyer, M.C.T., Riehle, M., Hayashi, J., Scholl, M., Sprössler, C., Britland, S.T., Offenhaeusser, A., Knoll, W., 1999. Bioassay development: the implications of cardiac myocyte motility in vitro. In Vitro Cell. Dev. Biol.-Anim. 35, 352–356.

Douglas, M.A., 1989. U.S. Patents 4855017.

Ewald, D., Van Den Berg, A., Grisel, A., 1990. Technology for backside contacted pH-sensitive ISFETs embedded in a p-well structure. Sens. Actuators B-Chem. B1 (1–6), 335–340.

Fromherz, P., 1999. Extracellular recording with transistors and the distribution of ionic conductances in a cell membrane. Eur. Biophys. J. 28, 254–258.

Fromherz, P., Offenhäusser, A., Vetter, T., Weis, J., 1991. A Neuron–Silicon Junction: a Retzius cell of the leech on an insulated-gate field-effect transistor. Science 252, 1290–1293.

Higgins III, L.M., Gentile, J.C., Beddingfield, S.C., 1998. U.S. Patent US5710071.

Ingebrandt, S., 2001. Characterisation of the cell-transistor coupling. Ph.D. Thesis. Johannes-Gutenberg-Universität, Mainz, Germany (http://archimed.uni-mainz.de/).

Ingebrandt, S., Yeung, C.K., Krause, M., Offenhäusser, A., 2001. Cardiomyocyte-transistor-hybrids for sensor application. Biosen. Bioelectron. 16, 565–570.

Jansseune, L., Brand, R., 1998. World Patent WO9813863.

Krause, M., Ingebrandt, S., Richter, D., Denyer, M., Scholl, M., Sprössler, C., Offenhäusser, A., 2000. Extended gate electrode arrays for extracellular signal recordings. Sens. Actuators B 70, 101–107.

Laermer, F., Schilp, A., 1999. German Patent DE19826382A.

Lau, J.H., 1995. FLIP-CHIP Technologie. McGraw-Hill, New York, p. 223.

Merlos, A., Esteve, J., Acero, M.C., Cane, C., Bausells, J., 1995. Application of nickel electroless plating to the fabrication of low-cost backside contact ISFETs. Sens. Actuators B-Chem. B27 (1–3), 336–340.

Offenhäusser, A., Sprössler, C., Matsuzawa, M., Knoll, W., 1997. Field-effect transistor array for monitoring electrical activity from mammalian neurons in culture. Biosens. Bioelectron. 12 (8), 819–826.

Osorio-Saucedo, R., Luna-Arredondo, E.J., Calleja-Arriaga, W., Reyes-Barranca, M.A., 1996. New chemical sensor based on a MOS transistor with rear contacts and two flat surfaces. Sens. Actuators B-Chem. B37 (3), 123–129.

Powell, R.A., 1987. U.S. Patent US4661177.

Regehr, W.G., Pine, J., Cohan, C.S., Mischke, M.D., Tank, D.W., 1989. Sealing cultured invertebrate neurons to embedded dish electrodes facilitates long-term stimulation and recording. J. Neurosci. Methods 30, 91–106.

Simon, J., Reichl, H., 1990. Single chip bumping for TAB. Proceedings of 2nd International TAB-Symposium ITAB '90, San Jose, p. 4.

Sprössler, C., Denyer, M., Britland, S., Knoll, W., Offenhäusser, A., 1999. Electrical recordings from rat cardiac muscle cells using field-effect transistors. Phys. Rev. E 60 (2), 2171–2176.

Sprössler, C., Richter, D., Denyer, M., Offenhäusser, A., 1998. Long-term recording system based on field-effect transistor arrays for monitoring electrogenic cells in culture. Biosens. Bioelectron. 13, 613–618.

Stern, M.B., Medeiros, S.S., 1992. Deep three-dimensional microstructure fabrication for infrared binary optics. J. Vac. Sci. Technol. B 10 (6), 2520–2525.

Thiébaud, P., Lauer, L., Knoll, W., Offenhäusser, A., 2002. PDMS device for patterned application of microfluids to neuronal cells arranged by microcontact printing. Biosen. Bioelectron. 17, 87–93.

Van Den Vlekkert, H.H., Kloeck, B., Prongue, D., Berthoud, J., Hu, B., De Rooij, N.F., Gilli, E., De Crousaz, P., 1988. A pH-ISFET and an integrated pH-pressure sensor with back-side contacts. Sens. Actuators 14 (2), 165–176.

Yeung, C.K., Ingebrandt, S., Krause, M., Offenhäusser, A., Knoll, W., 2001. The validation of the potential use of field effect transistors in pharmacological bioassays. J. Pharmacol. Toxicol. Meth. 45, 207–214.

Yeung, C.K., Ingebrandt, S., Krause, M., Sprössler, C., Denyer, M., Britland, S.T., Offenhäusser, A., Knoll, W., 2000. Investigations into the use of miniaturised field effect transistors (FETs) as a novel electrophysiological tool in pharmacological research. Br. J. Pharm. 131 (S), 217.